

## Growth and Optical Study of Carbon Nanotubes in a Mechano-Thermal Process

Mohd Rafie Johan\*, Lim Siang Moh

Nanomaterials Engineering Research Group, Advanced Materials Research Laboratory, Department of Mechanical Engineering,, University of Malaya, Lembah Pantai, 50603 Kuala Lumpur, Malaysia

\*E-mail: [mrafiej@um.edu.my](mailto:mrafiej@um.edu.my)

*Received:* 2 March 2012 / *Accepted:* 19 November 2012 / *Published:* 1 January 2013

---

Carbon nanotubes (CNTs) are synthesized by mechano-thermal method. The graphite was milled in air atmosphere and subsequently annealed. The samples were characterized by XRD, SEM, TEM, UV-vis spectrometer and FTIR. The TEM result showed that the CNTs has open and close-end structure. Two different growth mechanisms were proposed for both structures. The absorption spectra were slightly decreases and shifted to the longer wavelength. The optical bandgap for CNTs is 4.2 eV. FTIR spectrum detected two CH<sub>2</sub> functional group and thought to exist at tips of the CNTs.

---

**Keywords:** Carbon nanotubes; Mechanical milling; Annealing; Optical bandgap; Functional group

### 1. INTRODUCTION

Since the discovery of carbon nanotubes (CNTs) in 1991 by Iijima [1], this new form of carbon has shown promising potential for application in many engineering fields due to their many unusual properties. Long CNTs are required to be used for some electronic and structural applications. The longest CNTs have length up to several tens centimeters [2,3]. However, short nanotubes with open tips is needed for other application such as chemical or energy storage [4,5]. The open tips facilitated atomic or ionic diffusion and chemical reactions while the close tip hinders diffusion into the tube interior. One of the important challenges in CNTs application lies in shortening and opening of CNTs to attain novel mechanical, chemical and transport properties. Quite evidently, when these applications go to an industrial stage, a large quantity of nanotube materials is required. However, high yield and quality nanotubes are still not available in large quantities. Their production costs are also very high [6]. Several methods have been attempted to get large quantity and low cost production. Among them, mechano-thermal process seems to be the simplest process for producing large quantity CNTs [7]. The

mechano-thermal process consists of mechanical milling and thermal annealing process. Besides, the milling process has been able to get short and open ended CNTs [8]. Although CNTs have been observed in milled graphite samples after annealing [9], we propose here the formation mechanism for CNTs in a milled graphite sample after annealing. We also investigate the optical properties of the CNTs.

## 2. EXPERIMENTAL PROCEDURE

Crystalline hexagonal graphite powders with a purity of 99.8% were mechanically ground at room temperature using a planetary ball mill after 150 hours. The rotating speed of the vial was 400 rpm. The milled samples were annealed in an alumina tube furnace under a nitrogen gas flow at 1400°C for 4 hours. The microstructure of the milled and annealed samples was investigated using X-ray Diffraction (XRD), Philips X' pert MRD diffractometer with CuK $\alpha$  radiation ( $\lambda = 1.54056\text{\AA}$ ), SEM (Philips x (-40) and

TEM (LEO 912 Omega). Optical properties were examined using UV-VIS spectroscopy (UVIKON 923 Double Beam UV-VIS spectrometer). The chemical functionalization was determined using FTIR (Bruker IFS66V/S).

## 3. RESULTS AND DISCUSSION

### 3.1. XRD analysis

Fig. 1 shows the XRD patterns of as-received, milled and annealed samples.

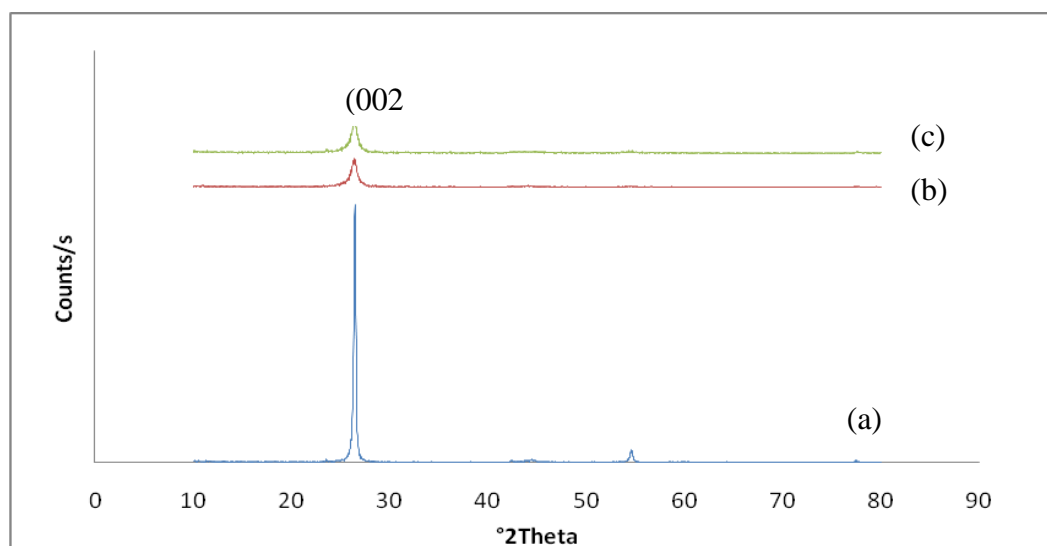


**Figure 1.** X-ray diffraction spectra of graphite sample: (a) as-received; (b) after 150 hours milling; (c) after annealing

The 2 $\theta$  diffraction peaks at 26.6° is attributed to the (002) plane for the graphite powder [10]. The diffraction peak at 55° in Fig 1(a) is presumably the impurity of the as-obtained raw graphite. The similarity of the position of the (002) shows that the graphitization remains almost the same for all samples. It proves that the fracture is much localised. It can be seen that the intensity of (002) peak decreases for the milled sample as shown in Fig. 1 (b), while interestingly increases slightly after annealing due to recrystallization (Fig. 1(c) ). It is recognized that the three-dimension (3D) orders of crystalline graphite powders are destroyed during the milling process [11]. The mechanism can be explained by the big mismatch of the very strong sp<sup>2</sup> C-C bonds that make up the graphene planes with the weak Van Der Waals forces that hold these planes together. Preferential cleavage along the weak bonds combined stacks in c-axis direction but not the strong network of parallel to planar planes. Samples that has been milled for a long period of time (150 hours) do not result in an amorphous phase but form a better ordered crystallize structure. This is corresponding to long range reorganization of graphite interlayer along the c-axis from nanostructured graphite. A noticeable peak broadening occurred for the milled and annealed samples indicated the reduction of crystallite size as calculated from Scherer formula and listed in Table 1.

**Table1.** The crystallite size and band gap energy as-received, 150 milling and annealing samples.

Sample	Crystallite size (nm)	Band gap energy (eV)
As-received powder	35	5.2
Milled for 150 h	13	4.8
Annealed	15	4.2

### 3.2. SEM analysis

Figs. 2 - 4 show the SEM micrograph for as-received, milled and annealed samples.

Compared with the as-received sample, the graphite particle has been broken into small size by mechanical force after 150 hour milling in air atmosphere. It can be seen that the sizes of particles are reduced into a wide range of size distribution from hundreds of nanometers to several microns in the form of aggregates. On one hand, the graphite particles split as result of the important internal strain created by the high pressure applied to the grains. On the other hand, the highly divided particles tend to agglomerate due to the high reactivity of their surfaces in order to minimize the surface energy [12]. The particles become highly agglomerated after the annealing process as shown in Fig. 4.

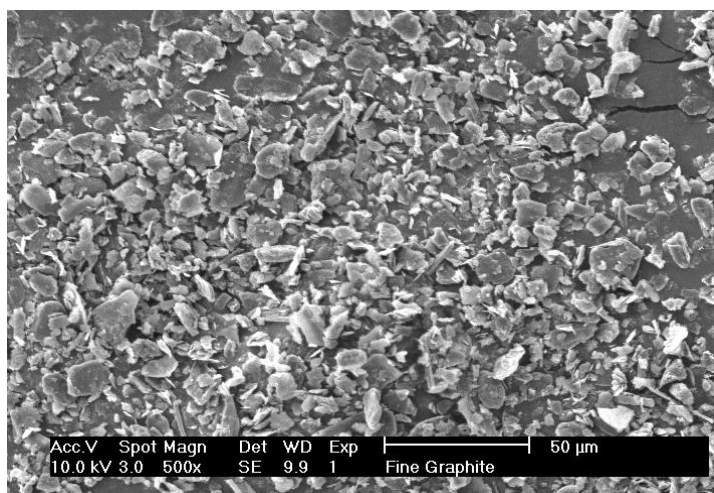


**Figure 2.** SEM micrograph of as-received sample

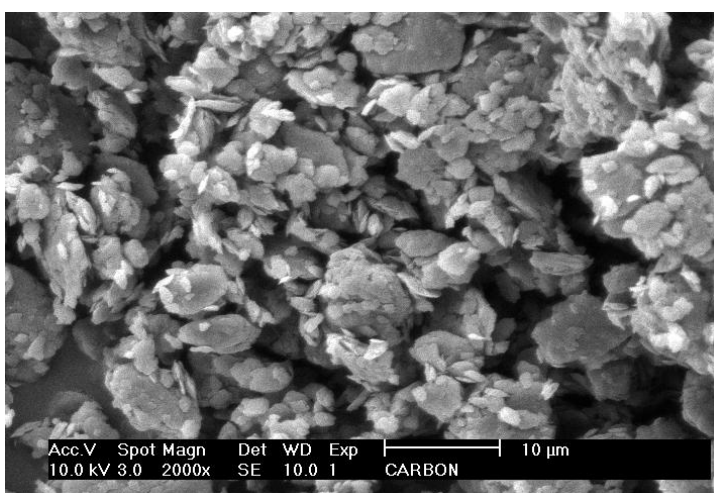


**Figure 3.** SEM micrograph of milled sample

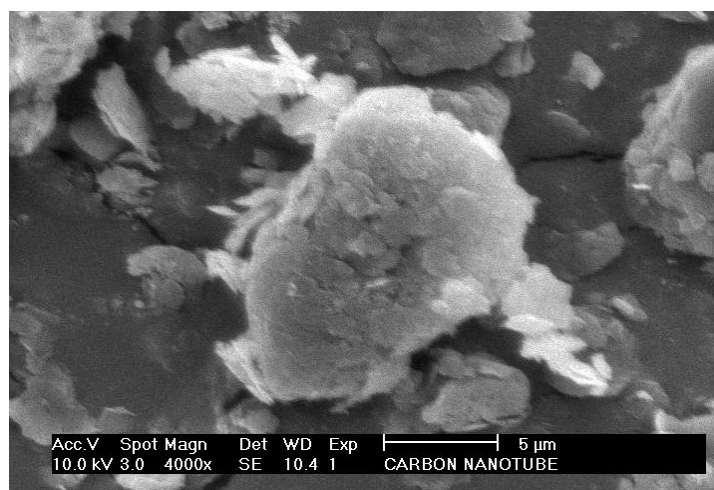


**Figure 4.** SEM micrograph of annealed sample

## 3.5. TEM analysis

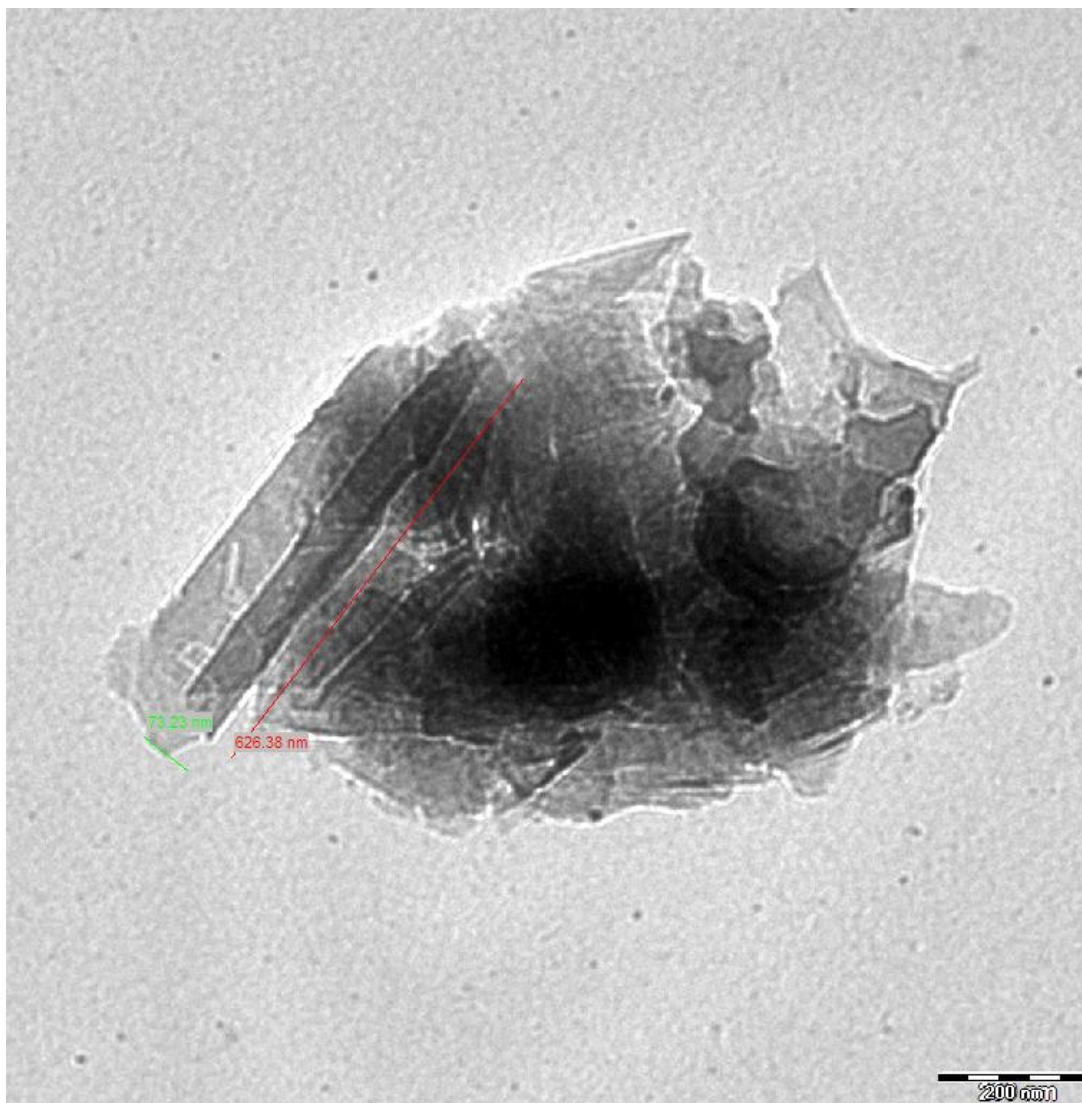


**Figure 5.** TEM image of open-ended analysis CNT

Clusters containing of CNTs were found in a annealed graphite sample. A typical TEM micrograph taken from the edge of an image nanotube cluster is shown in Fig. 5. These CNTs have an open-end with diameter and lengths are 73 and 626 nm, respectively.

Fig. 6 shows the TEM image of close end CNTs with diameter and length are 42 and 182 nm, respectively. Most CNTs have one free end with the other connected to a cluster of carbon particles suggesting that nanotubes grow out radially from the carbon clusters.

By analyzing the TEM image, we can deduce that nanotubes might be form from two different growth mechanisms. This suggests different types of CNTs can be produced by mechano-thermal process. In open-end growth mechanism, both end of nanotube remains open and without attachment of cap during growth process. Free carbon atoms are supplied and added to the ends of nanotube. The sequential absorption of  $C_2$  dimer will form hexagon and added to the open end. This will result continuous growth of nanotube in needle axis. However, any absorption of  $C_3$  trimers will form

pentagon at the dangling end of open end. The introduction of pentagons will cause positive curvature which would start a capping of nanotube and terminate the process. Sometime the addition of pentagons at the open end will leads to the changes of size or orientation of nanotube. Thus, any introduction of pentagon would causes bending or curvature of nanotube. The free end nanotube remains close and tube end connected to a cluster of disorder carbon source in the closed end mechanism.

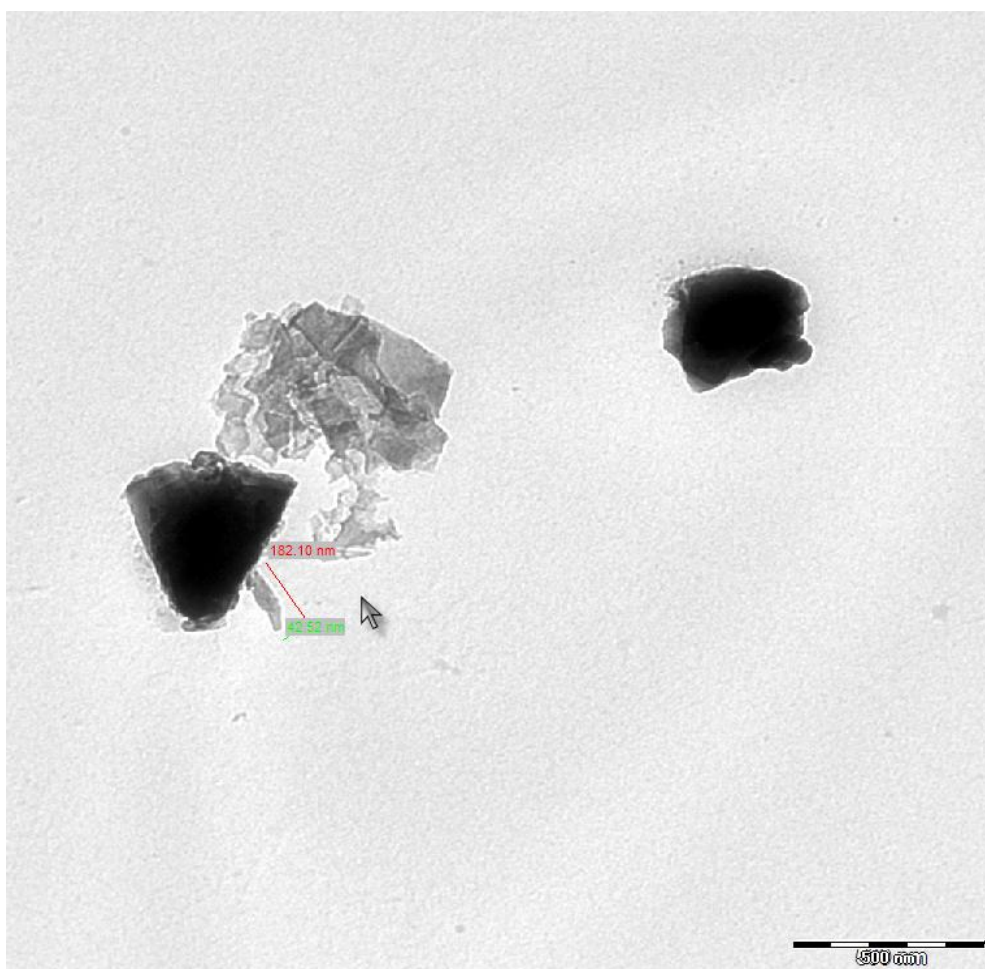


**Figure 6.** TEM image of close-ended analysis CNT

The continuous longitudinal growth of nanotube may be due to the addition  $C_2$  dimer which supplied by disorder carbon source. The bending of nanotube will due to absorption of  $C_3$  trimers which similar to the open-end mechanism. The main different between open and close end mechanism are due to the attachment of cap and attachment of tube.

### 3.6. UV – vis studies

Fig. 7 shows the absorbance spectra of as-received, milled and annealed sample.



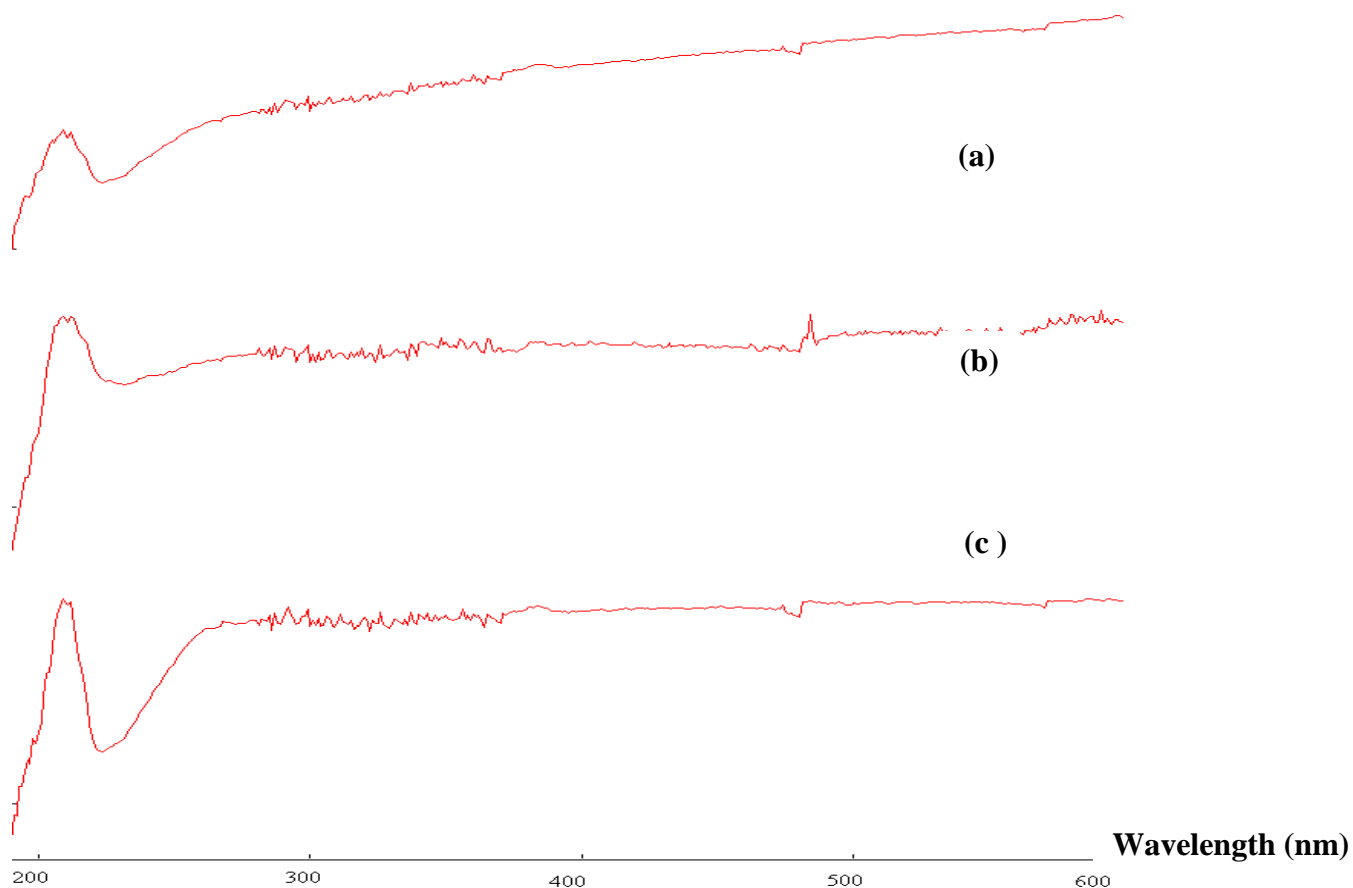


**Figure 7.** UV-vis spectra of (a) as-received, (b) milled and (c) annealed sample.

The corresponding spectra for all samples show a similar development. It indicates that the UV-vis spectra obtained are specific for the CNTs studied. For milled and annealed samples, the absorbance gradually decreases and the peaks were slightly moved to the longer wavelength. This is partly due to scattering, especially in the lower wavelength range. In order to evaluate the optical band gap energy, the absorption coefficient have been determined from the spectra using the Tauc relation [14]

$$\alpha = [A (h\nu - E_g)^{1/2}] / h\nu \quad (1)$$

where A and  $E_g$  is a constant and optical bandgap respectively. Plots of  $(\alpha h\nu)^2$  versus the photon energy ( $h\nu$ ) in the absorption region near the fundamental absorption edge indicate direct allowed transition in the material as shown in Figs. 8-10. The optical band gap was estimated from the extrapolation of the linear portion of the graph to the photon energy axis. It is shown in Table 1 that  $E_g$  decreases for milled and annealed samples. This may due to the possibility of structural defects in the samples during milling and annealing, which could give rise to the allowed states near the conduction band in the energy bandgap.

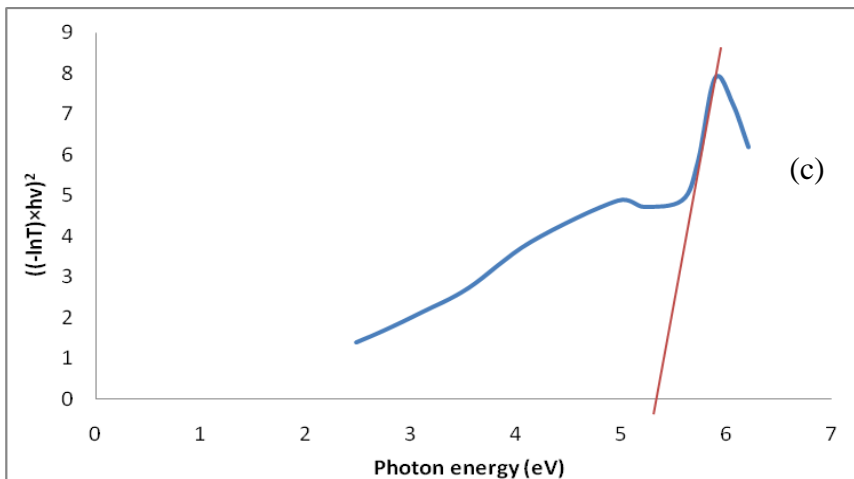


**Figure 8.** Tauc's plot for as-received sample

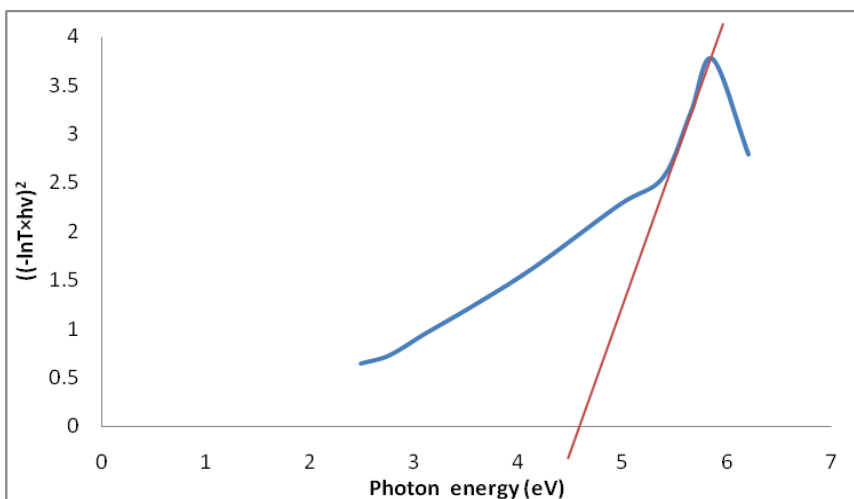


**Figure 9.** Tauc's plot for milled sample

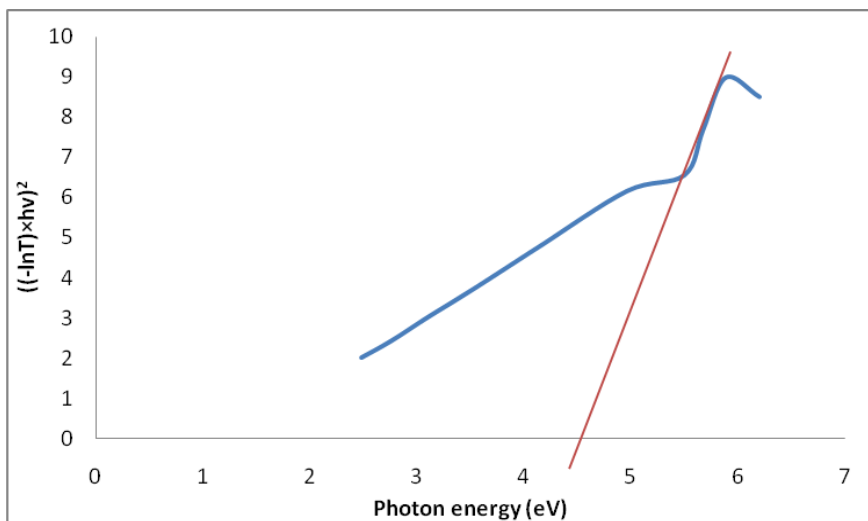


**Figure 10.** Tauc's plot for annealed sample



### 3.8. FTIR Analysis

The FTIR spectrum of CNTs is shown in Fig.11.

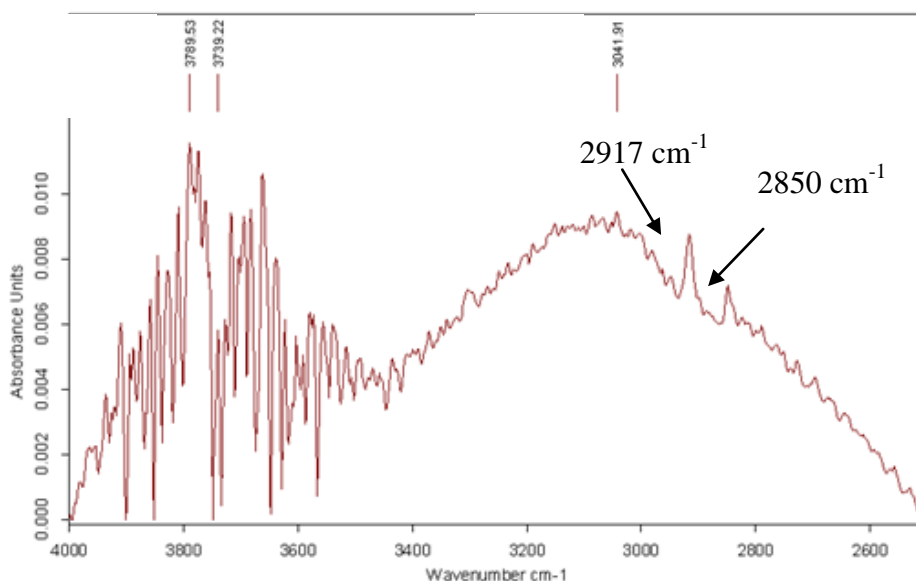


**Figure 11.** FTIR spectrum of annealed sample ( $2500\text{ cm}^{-1} - 4000\text{ cm}^{-1}$ )

The bands at 2917 and 2850  $\text{cm}^{-1}$  are due to asymmetrical and symmetrical stretching of  $-\text{CH}_2$  bonds, respectively [13]. Only very small quantity of  $-\text{CH}_2$  functional group was detected. From the small peak intensity, they are thought to exist at tips of the CNTs. However, we cannot deny the possibility of being dangled from the surface of nanoparticles.

## 4. CONCLUSION

Dual type of (open and close end) CNTs were successfully produced through the mechano-thermal process. In the open end CNTs, both ends of nanotubes are without cap attachment during growth. Meanwhile, pentagon was introduced for close end CNTs and causes bending to the nanotube. The optical bandgap of CNTs is higher than the graphite powder due to defect and scattering during milling and annealing. Very small quantity of  $\text{CH}_2$  functional groups was detected and thought to exist at the tips of the CNTs.

## ACKNOWLEDGMENTS

The financial support received from UMRG (RG038/09AET) University of Malaya is gratefully acknowledged.

## References

1. Iijima S. (1991). Helical microtubules of graphitic carbon. *Nature*. 354. 56–8.
2. H.W.Zhu, C.L Xu, D.H. Wu, B.Q. Wei, R,Vajtai, P.M Ajayan, *Science* 296 (2002) 884-886.
3. M.D. Lay, J.P Novak, E. S. Snow, *Nano Lett.* 4(4) (2004) 603-606

4. J.Chen, M.A Namon, N.Nu, Y.S.Chen, A.M Rao, P.C Eklund, R.C Nadden, *Science* 282 (1998) 95-98.
5. K.Awasthi, R. Kamalakarm, A.K Singh O.N, Srivastava, *Int. J. Nydr. Energy* 27 (4) (2002)
6. P.Ajayan, O.Z.Zhou, *Topics in Applied Physics* Vol.80, Springer-Verlage, Berlin, Heidelberg 2001 p.39
7. Y.Chen, M.J Conway, J.D Fitzgerald, *Allp.Phys.A* 76, 633-636 (206)
8. J.H Ahr, H.S Shin, Y.J.Kim, H. Chung, *J.All Comp.* 434-435 (2007) 428-432.
9. Y.Chen, L.T Chadderton, J.S Williams, J. Fitzgerald, *Marter.Sci.Forum* 343-346, 63 (2000)
10. T.S Ong, H.Yang, *Carbon* 38 (2000) 2077-2085
11. T.Fukunaga, K.Nagoro. H.Mizutari, H.Wakayama, Y.Fukuohima, *J.Nanocrystal. Solids* 232-234 (1998) 416-420
12. R.Jarot, D.Guerand, *Prog.Master Sci.* 50 (2005) 1-42
13. L, Jiang, L. Guo, J. Sun, *J.Coll.Int.Sci*, 260 (2003) 89-94
14. P.P Sahay, S.Tewari, R.K.Nath, *Cryst.Res.Technol.* 42 7 (2007) 723-729